

**Antiferromagnetic ordering on the frustrated fcc lattice in the intermetallic compound GdPtBi**

Sergii Khmelevskiy

*Center for Computational Material Science, Institute of Applied Physics, Vienna University of Technology, Makartvilla, Gusshausstrasse 25a, 1040 Vienna, Austria*

(Received 29 May 2012; revised manuscript received 13 August 2012; published 24 September 2012)

The type of antiferromagnetic magnetic order in the half-Heusler intermetallic compound GdPtBi, where the Gd atoms form a magnetically frustrated fcc lattice, has been investigated using exchange constants calculated from first principles within the framework of the Green's function based magnetic force theorem. It is found that the degeneracy of the magnetic states on the fcc lattice with antiferromagnetic nearest neighbor interaction is removed by strong fourth-nearest neighbor interaction along the cube diagonal. We show that an antiferromagnetic ordering of so-called "third kind" occurs at low temperatures. The Monte Carlo simulations using our derived exchange constants predict an experimental Néel temperature ( $T_N$ ) with good accuracy. The estimated temperature dependence of the correlation functions in the paramagnetic region exhibit a typical behavior for a frustrated system—a massive short-range order is retained for temperatures which are one order of magnitude higher than  $T_N$ .

DOI: [10.1103/PhysRevB.86.104429](https://doi.org/10.1103/PhysRevB.86.104429)

PACS number(s): 75.25.-j, 75.10.Jm, 71.15.Mb, 75.30.Et

**I. INTRODUCTION**

A recent extensive search for novel topological insulators bring close attention to the half-Heusler compounds with three-valence rare earth atoms as one of the constituents. It has been predicted in particular that GdPtBi with well localized  $4f$ -magnetic moments may be a magnetic topological insulator.<sup>1</sup> However, recent experimental angle-resolved photoemission spectroscopy (ARPES) studies did not reveal any topologically nontrivial behavior in this material,<sup>2</sup> although the ARPES results can be very well correlated with calculated band structures derived within a framework of the local-spin density approximation (LSDA).<sup>2</sup> A number of LSDA studies, including also GGA (general gradient approximation) and LSDA +  $U$ , have been published recently with certain conclusions drawn on possible mechanisms which may lead to a topological insulator behavior.<sup>3,4</sup> In those studies the band structure of GdPtBi has been investigated for the ferromagnetic state or even for a nonmagnetic one. Although there is no experimental validation of topological insulating behavior in GdPtBi, even the theoretical discussion of such a possibility requires the knowledge about the exact symmetry of the magnetic ground state, as it has been recently shown recently by Mong *et al.*<sup>5</sup> in their theory of antiferromagnetic topological insulators. However, the question about the magnetic ground state in GdPtBi remains open. The original experimental investigation<sup>6</sup> of this compound has revealed a sharp magnetic phase transition at a temperature of about 9 K without net magnetization at temperatures below, thus suggesting an antiferromagnetic ordering of the Gd moments in the ground state. Since in the half-Heusler structure (see Fig. 1) magnetic Gd atoms form an fcc magnetic lattice and there exists an experimental signature of antiferromagnetic order, it appears that the problem of magnetic order in GdPtBi has a nontrivial interest in its own right since the fcc lattice is geometrically frustrated.

Magnetism in frustrated systems is a subject of great interest during the past decades due to a number of intriguing phenomena, such as, for example, formation of spin-ice or spin-liquid states due to a highly degenerate magnetic ground

state.<sup>7</sup> One topic of special interest is the effect of magnetic frustration in metallic systems (for a recent review see Ref. 8).

There exist a number of special effects which are theoretically predicted but not yet observed,<sup>8</sup> since in particular there are not many metallic materials with frustrated ground state available. In metallic magnets the degeneracy of the ground state is often removed by long-range magnetic interactions. These interactions in metals are usually much stronger than in insulators since the indirect interaction is mediated by the conduction band. However, even if the degeneracy of the ground state is removed, the results of the combination of geometrical frustration and the competition between distant interactions may lead to the formation of the exotic magnetic ordering, massive short-range order effects above magnetic critical temperature, etc. All together this may lead to a nontrivial temperature dependence of various response functions like, for example, resistivity. The determination of these exotic magnetic phases and the mechanism leading to their stabilization is a formidable task, which saw a lot of effort during the past decades.<sup>9</sup> Let us note also that the competition between distant interactions may be the source of the frustration effects by itself.<sup>10</sup>

An important example of the geometrically frustrated lattice is fcc, formed by magnetic Gd atoms in the half-Heusler structure (Fig. 1). In a number of theoretical works the behavior of a Heisenberg Hamiltonian with antiferromagnetic first and second nearest neighbors (NN) interactions on a fcc lattice has been studied<sup>11–13</sup> with particular emphasize on the phase stabilities and the mechanisms removing the spin degeneracy. The practical interest in studying the antiferromagnetic state on a fcc lattice originates, in particular, from the still unresolved problem of the magnetism of fcc Fe. This problem is also related to the explanation of the phase transformations and stability of austenitic steels. There exist a number of investigations, including *ab initio* simulations, to understand the ground state properties of fcc Fe, which seems to be rather complex.<sup>14,15</sup> The rather unusual classical and quantum spin dynamics has been studied in the frustrated fcc antiferromagnet NiS<sub>2</sub>.<sup>16</sup> This latter material is not metallic and has strongly

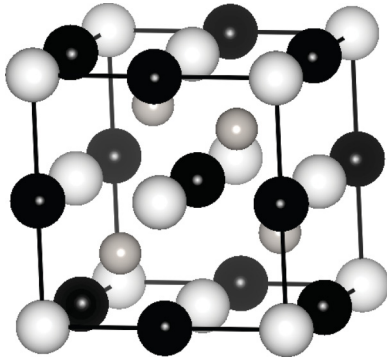


FIG. 1. Crystal structure of GdPtBi. Light balls: Gd atoms, dark balls: Bi, and gray balls: Pt. Gd atoms form fcc lattice.

localized Ni moments, which allows for a good description in the framework of a quantum Heisenberg model. It is in contrast to metallic fcc Fe, which is an itinerant ferromagnet and its spin dynamics can hardly be described with a Heisenberg Hamiltonian. Moreover, theoretical predictions concerning the magnetic ground state of fcc Fe cannot directly be verified experimentally since one cannot stabilize this structure at low temperatures.<sup>17</sup> It thus seems that GdPtBi is a suitable material to study the problem of magnetic frustrations on a fcc lattice since it is metallic and exhibits a strong localization of gadolinium  $4f$  moments allowing for the application of the Heisenberg model.

## II. MODEL AND METHODOLOGY

To discuss magnetic order in GdPtBi we calculate the interatomic magnetic exchange interactions from first principles using the Green's-function based magnetic-force theorem (or so-called Liechtenstein method).<sup>18</sup> A particular implementation of this technique used here is based on the electronic structure calculation using the scalar relativistic Korringa-Kohn-Rostoker Green's function method in the atomic sphere approximation (KKR-ASA)<sup>19,20</sup> as described in Ref. 21 within the framework of the local spin density approximation.<sup>22</sup> This procedure allows us to calculate<sup>18,21</sup> the exchange constants  $J_{ij}$  of a classical Heisenberg Hamiltonian

$$H = - \sum_{i,j \in \{Gd\}} J_{ij} \vec{e}_i \vec{e}_j, \quad (1)$$

where the summation is over Gd sites of the fcc lattice (Fig. 1) and  $\vec{e}_i$  are the unit directional vectors of the magnetic moment on  $i$ th lattice site. In earlier works this scheme was successfully applied to the calculations of the exchange constants in pure hcp Gd<sup>23,24</sup> and bcc Eu<sup>25</sup> metal providing a qualitative explanation of the magnetic ground state (spin spiral state in Eu) as well as excellent quantitative results for the respective Néel temperatures.

Similarly to the cited works<sup>24,25</sup> on pure Gd and Eu, we applied here an open-core approximation to treat the  $4f$ -electronic state of Gd, where the occupation of spin-split  $4f$ -core levels was chosen such that the magnetic moment of the atomic core states is equal to  $7 \mu_B$  as in the ground state of the free Gd<sup>3+</sup> ion. This simple open-core approach is particularly justified by the zero orbital moment of the

half-filled  $4f$  shell of Gd (in  $3^+$ ) and Eu in  $2^+$  valence states and consequently the negligible crystal field splitting effects on the localized  $4f$  states. For further details on the justification of this approximation we refer to original papers.<sup>26,27</sup>

The derived exchange constants show robustness with respect to choice of atomic ratio of the ASA method. Thus we apply a more natural choice of equivalent spheres for Gd, Pt, Bi atoms, including also empty spheres placed at the vacant position in half-Heusler structure. More important is the fact that the value of the exchange constants almost do not depend on the reference magnetic state. They are almost the same in the ordered magnetic state (antiferromagnetic or ferromagnetic) and in the disordered local moment (DLM) state, which we adopt to model spin disordered paramagnetic state above the Néel temperature. Thus it appears that the magnetism in GdPtBi is even more suitable for a description in the framework of the Heisenberg model than pure hcp Gd (see detailed discussion of the application of DLM to pure Gd in Ref. 24).

In this work we use DLM as reference for the magnetic state. A self-consistent electronic structure has been calculated using 4047  $k$  points in full Brillouin zone (IBZ) and 182 205  $k$  points were used for the calculation of the exchange constants. The  $spd$ -valence band was calculated using a basis function expansion up to  $l_{\max} = 2$ . Multipole moment contributions to the nonspherical part of the electrostatic contribution to the one electron potential inside the ASA spheres were also determined by carrying out the summation up to  $l_{\max}^M = 5$ . The experimental<sup>6</sup> lattice constant of  $a = 6.71 \text{ \AA}$  is used for all calculations.

## III. RESULTS AND DISCUSSION

Similar to the case of pure Gd metal a spin polarization of the Gd valence electronic states locally persists in GdPtBi and also in the paramagnetic state. The calculated values of these moments in DLM state is  $0.17 \mu_B/\text{Gd}$ , resulting in  $7.17 \mu_B/\text{Gd}$  taking into the account localized  $4f$  electrons. The existence of the local spin polarization of the conduction bands in spin-disorder paramagnetic states was confirmed by ARPES studies for pure Gd.<sup>28</sup> Earlier it was shown<sup>29</sup> that DLM methods well described a mechanism leading to this polarization in hcp Gd. Here, however, the situation is slightly different from pure Gd since this polarization is less dependent on the magnetic state (e.g., in ferromagnetic state the calculated value is  $0.11 \mu_B/\text{Gd}$ ). This is due to the fact that the distance between the Gd atoms in the half-Heusler structure is much larger than in pure Gd, thus there is no direct hybridization of  $spd$  states of the Gd atoms. Small variations due to changes of the magnetic state are mainly reasoned in the hybridization of the Gd valence states and the nonmagnetic Bi and Pt. This is the main reason why the exchange constants show much more robustness with respect to the reference magnetic state than in pure Gd and consequently allow a better applicability of the Heisenberg model to describe the magnetic thermodynamics of this system.

In Table I we present the calculated exchange constants of the Hamiltonian [Eq. (1)] for the first nine nearest-neighbor (NN) shells in the fcc structure. The remaining ones, including the omitted seventh and eighth NN interaction, have values less

TABLE I. Calculated exchange constants of the Heisenberg Hamiltonian [Eq. (1)] for the nearest neighbor shells on a fcc lattice. In the first row the corresponding cubic translation vectors are given. The number of the nearest neighbor atoms in the respective shell is specified in the second row.

	1NN 0,1/2,1/2	2NN 0,0,1	3NN 1/2,1/2,1	4NN 1,1,0	5NN 0,1/2,3/2	6NN 1,1,1	9NN 0,3/2,3/2
$J_{ij}$ , mRy	-0.061	0.004	-0.004	-0.011	-0.001	-0.001	-0.002
Number of NN	12	6	24	12	24	8	12

than 1  $\mu$ Ry being essentially at the verge of computational accuracy. According to the definition of our Hamiltonian [Eq. (1)] a negative sign of  $J_{ij}$  means antiferromagnetic interaction. One can see immediately that the dominating interaction is antiferromagnetic for the first nearest neighbor, which alone will produce an infinite degeneracy of the magnetic ground state on the fcc lattice. On a fcc lattice it is impossible to arrange an antiferromagnetic structure that would have solely AFM nearest neighbor bonds (geometrical frustration). What makes a selection of the ground state is more distant interactions, among which most important is the fourth nearest neighbor AFM interaction, and to some extent the third NN one, which is less strong than the fourth but has 24 atoms in the respective coordination shell (against 12 in the fourth coordination shell—see Table I).

Basically there are possibly five “kinds” of different collinear antiferromagnetic arrangements on the fcc lattice (see Ref. 11 for details). We perform Monte Carlo (MC) simulations using a Hamiltonian with the first nine NN interactions as presented in Table I. The MC simulation has been performed applying the Metropolis algorithm on a  $20 \times 20 \times 20$  fcc unit cell with more than  $10^5$  MC steps for equilibration and averaging. To check the stability of the results with respect to the periodical boundary conditions we use a couple of smaller lattice sizes also. The simulations show that the low temperature antiferromagnetic phase is of the “third kind” according to definitions given in Ref. 11. This structure is presented in Fig. 2. The magnetic unit cell of this structure is a simple tetragonal which includes two simple cubic unit cells of the original fcc structure. The stabilization of this structure can be understood by considering the number of spin-up (filled balls in Fig. 2) and spin-down atoms in the respective shells surrounding a central, say spin-up, atom and considering the exchange parameters from Table I. In

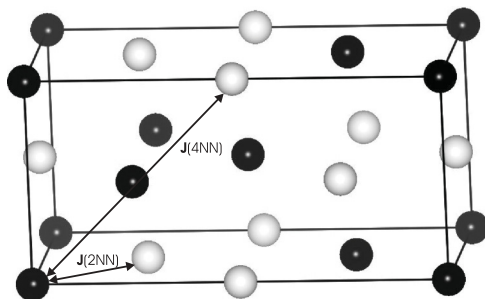


FIG. 2. Antiferromagnetic arrangement of Gd moments of the third kind on fcc lattice. Dark and light balls are atoms with spin-up and spin-down moments. Arrows show two strongest pairwise 1NN and 4NN exchange interactions.

the first nearest neighbor shell this central atom has 8 out of 12 neighbors with antiparallel and 4 with parallel spin. The fcc structure cannot do better on average to satisfy the strongest 1NN antiferromagnetic coupling. The second strongest interaction is the 4NN along the cube face diagonal and is also antiferromagnetic (see Fig. 2). The magnetic structure shown in Fig. 2 provides all 8 AFM and 4 FM neighbors on the respective shell. This is the main factor, which determines the stability of third kind AFM structure in GdPtBi since the other four kinds of possible AFM structures on the fcc lattice<sup>11</sup> do not provide such auspicious conditions for the strongest interactions in GdPtBi. We also note that the second NN interaction, which are mainly considered in theoretical papers on the frustration in fcc lattices, is very weak in GdPtBi. Moreover, it has an opposite sign to the 1NN interactions and thus cannot stabilize a noncollinear ground state.<sup>13</sup> In order to illustrate this point we plot in Fig. 3 the Fourier transform of the calculated exchange interactions taken up to the 21 NN shell (although the interactions starting from the tenth NN shell are very small) along selected directions in the reciprocal space. We found that its maxima correspond to the commensurate  $q = 2\pi(0, \frac{1}{2}, 1)$  wave vector, what is exactly the periodicity of the collinear spin structure of the third kind which appeared at low temperatures in the MC simulations. This structure is built of four ferromagnetic layers stacking in the [012] direction in the sequence “spin-up-up-down-down.”

We have also performed direct total energy LSDA calculations considering a couple of possible collinear antiferromagnetic structures on fcc lattice, namely those which

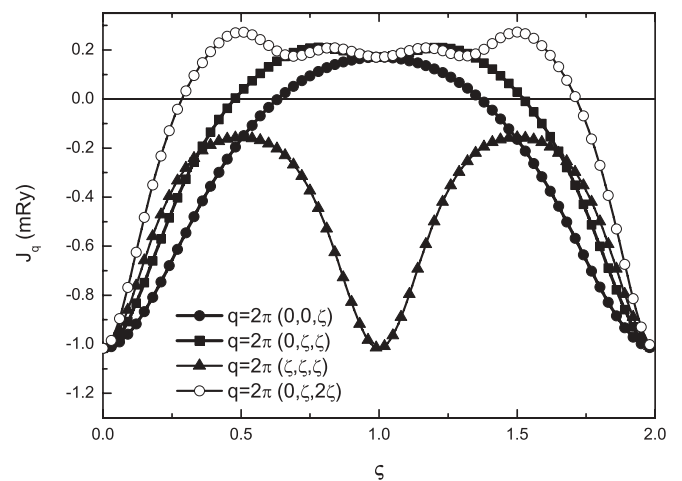


FIG. 3. Fourier transform  $J(q)$  of exchange interactions of Hamiltonian (1) with 21 first NN shells. Open symbols are the direction providing the maximum value at  $q = 2\pi(0, \frac{1}{2}, 1)$ .

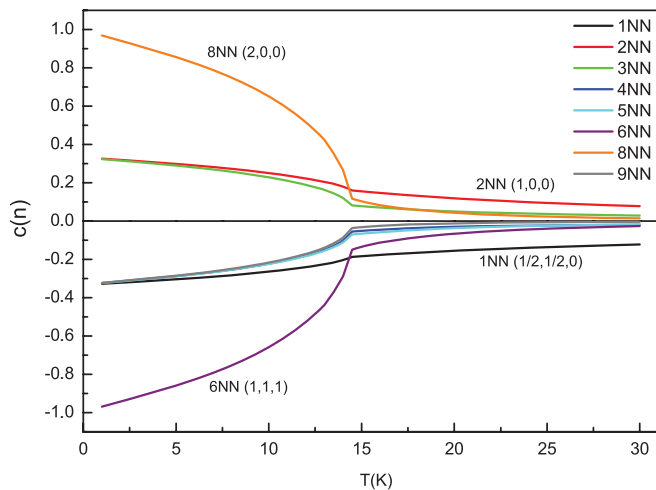


FIG. 4. (Color online) Calculated spin-spin correlation functions for GdPtBi for first  $n$ th NN (nearest neighbor) shells. Low temperature region.

are referred in, for example, Ref. 11, as ordering of first to fourth kind AFM ordering on fcc lattice. We found that they are very close in energy (the energy difference is just an order of  $10 \mu\text{Ry}$  per crystallographic unit cell). Only after achieving the total energy convergence with respect to  $k$  points much better than this value, we found that the structure of the third kind is lower in energy than “first kind” (“up-down” order of ferromagnetic [100] layers) by  $12 \mu\text{Ry}$  per unit cell, whereas the other structures are higher in energy by  $50\text{--}60 \mu\text{Ry}$ . Let us note again, however, that the exchange interactions, presented in Fig. 4 and Table I, are calculated for the disordered local moments state, which is used as a model for the paramagnetic state above Néel temperature and thus provide information concerning the order-disorder transition at elevated temperature, rather than information concerning the energy balance between various ordered configurations at  $T = 0$  K.

Let us note also that we have found a small gap in the scalar relativistic density of state at the Fermi level in disordered local moment state ( $0.01 \text{ mRy}$ ), suggesting that in the true paramagnetic state above  $T_N$  the system is a narrow band semiconductor without involving the effects of spin-orbit coupling.

In the following we give some discussion of the magnetic short-range order effects in the GdPtBi, also with comparison to the case of antiferromagnetic ordering on a nonfrustrated lattice. We consider the usual definition of the spin-spin correlation functions for the  $n$ th nearest neighbor shell

$$c(n) = \frac{1}{N} \sum_i \langle \vec{e}_i \vec{e}_{i+R(n)} \rangle, \quad (2)$$

where  $R(n)$  is a translation vector of the  $n$ th shell and the summation runs over all lattice sites. These functions provide important information concerning the short-range order in the system. For a fully ordered structure, one notes that for the sixth and eighth [corresponding to  $R(8) = \{002\}$ ] shells the values of the corresponding  $c(n)$  are  $-1$  and  $+1$ , respectively. The other shells, with  $n < 12$ , have values of correlation function being either  $+1/3$  or  $-1/3$  since the number of atoms in these shells with spins opposite to the central atom is either

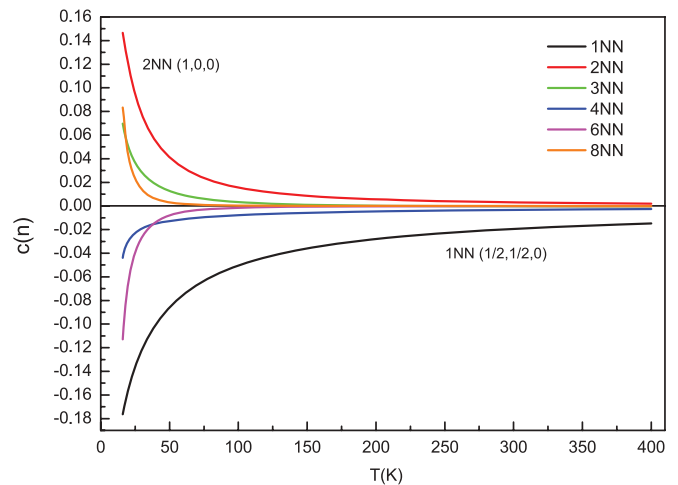


FIG. 5. (Color online) Calculated spin-spin correlation functions for GdPtBi for first  $n$ th NN (nearest neighbor) shells. High temperature region.

two times larger or smaller than the number of atoms with the same spin.

In Fig. 4 we present the temperature dependence of  $c(n)$  derived from the Monte Carlo simulations for the Hamiltonian (1) and the calculated exchange constants. First note that the predicted Néel temperature is at about 14 K, which is in fair agreement with the experiment<sup>6</sup> giving 9 K. The moderate disagreement with experiment may be a sign for the possible need of considering quantum effects in the Hamiltonian, despite that the Gd spin is rather high ( $S = 7/2$ ) and more close to the classical limit than any other magnetic substance.

The correlation functions given in Fig. 4 approach their limits corresponding to the ordered structure shown in Fig. 2 as temperature goes to zero. At the critical temperature (14 K) they considerably change their behavior. We find that the  $c(n)$  for the shortest range show a very slow decay above  $T_N$ . In Fig. 5 we plot their behavior at higher temperatures. One can see that massive short-range order is kept in the system up to a temperature which exceeds  $T_N$  by one order of magnitude. This behavior is typical for frustrated systems. The reason for it can be understood by taking into the account the rather large values of the interatomic exchange interactions, which in the absence of frustration would lead to a rather high critical temperature. For instance, if we change the sign of the 1NN interaction (ferromagnetic) the respective Curie temperature would be around 80 K (mean-field estimate). Thus strong short-range order effects develop in the system for temperatures much higher than the ordering temperature. The existence of such massive magnetic short-range order effects well above  $T_N$  would lead to various anomalous behaviors, for example, the resistivity, in a large temperature interval. Indeed, experimental results suggest a rather unusual temperature dependence of the resistivity<sup>6</sup> in GdPtBi, which may be due to magnetic short-range order effects.

In order to illustrate the difference between short-range order effects on frustrated fcc lattice in GdPtBi and the antiferromagnetic system on nonfrustrated lattice we have performed the MC simulation on simple cubic lattice with just one antiferromagnetic nearest neighbor interaction. The magnetic

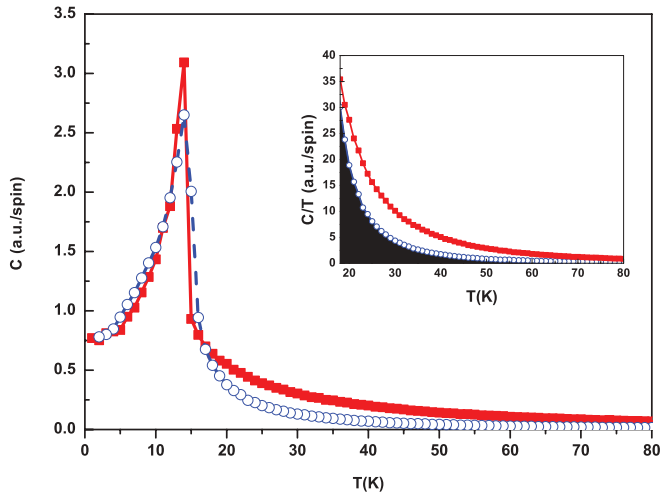


FIG. 6. (Color online) Magnetic specific heat from MC simulations with exchange interaction from Table I on fcc lattice (close squares) and on single cubic lattice with one NN exchange parameters equal to  $-0.032$  mRy (see text). Inset: the  $C/T$  ratio for the same simulations plotted above Néel temperature, an area under the curves is the magnetic entropy difference.

order at low temperatures is of simple “checkerboard” type, where all nearest neighbors of a given site of simple cubic lattice have opposite directions of the moment. The magnitude of the exchange interaction is chosen such to provide the same Néel temperature as we derived for GdPtBi in this work. The calculated magnetic specific heat ( $C_m$ ) for both cases is presented in Fig. 6. It is seen that short-range order effects

manifests themselves in much larger specific heat tail above  $T_N$  for frustrated GdPtBi than for simple cubic antiferromagnet. In particular, for the temperatures well above critical  $T \sim 3T_N$ , there is still a sizable magnetic contribution to the specific heat in the GdPtBi case, which is an order of magnitude larger than in the simple cubic nonfrustrated case. In the inset we plot the  $C/T$  ratio for both cases in the region above Néel temperature. The area under the respective curves is the contribution to the magnetic entropy from short-range order effects above  $T_N$ .

#### IV. CONCLUSIONS

We determine the magnetic ground state of GdPtBi to belong to the third kind of AFM on a fcc lattice (Fig. 2). Massive short-range order effects are taken place in a temperature interval well above Néel temperature. The key role in the stabilization of the ground state is played by fourth NN interactions along the cube face diagonal. Thus, it appears that GdPtBi is very well suited to study the effects of magnetic frustrations and further experimental verification is much desired. The low Néel temperature and the unusual behavior of the resistivity in this material also requires further theoretical consideration, calling also for a investigation of quantum effects in the Heisenberg Hamiltonian in a similar manner as previously studied<sup>11–13</sup> on some kinds of order on fcc lattices with a peculiar choice of the 2NN interaction.

#### ACKNOWLEDGMENT

The author acknowledges the support from the Austrian Science Fund (FWF) (SFB ViCoM F4109-N13).

- <sup>1</sup>S. Chadov, X. Qi, J. Kübler, G. H. Fecher, C. Lelsere, and S. C. Zhang, *Nat. Mater.* **9**, 541 (2010).
- <sup>2</sup>C. Liu, Y. Lee, T. Kondo, E. D. Mun, M. Caudle, B. N. Harmon, S. L. Bud’ko, P. C. Canfield, and A. Kaminski, *Phys. Rev. B* **83**, 205133 (2011).
- <sup>3</sup>W. Al-Sawal, H. Lin, R. S. Markiewicz, L. A. Wray, Y. Xia, S.-Y. Xu, M. Z. Hasan, and A. Bansil, *Phys. Rev. B* **82**, 125208 (2010); V. N. Antonov, P. Oppeneer, A. N. Yareshko, A. Ya. Perlov, and T. Kraft, *ibid.* **56**, 13012 (1997).
- <sup>4</sup>C. Li, J. S. Lian, and Q. Jiang, *Phys. Rev. B* **83**, 235125 (2011).
- <sup>5</sup>R. S. K. Mong, A. M. Essin, and J. E. Moore, *Phys. Rev. B* **81**, 245209 (2010).
- <sup>6</sup>P. C. Canfield, J. D. Thompson, W. P. Beyermann, A. Lacerda, M. F. Hundley, E. Peterson, and Z. Fisk, *J. Appl. Phys.* **70**, 5800 (1991).
- <sup>7</sup>R. Moessner and A. P. Ramirez, *Phys. Today* **59**, 24 (2006).
- <sup>8</sup>C. Lacroix, *J. Phys. Soc. Jpn.* **79**, 011008 (2010).
- <sup>9</sup>A. S. Oja and O. V. Lounasmaa, *Rev. Mod. Phys.* **69**, 1 (1997).
- <sup>10</sup>P. Chandra, P. Coleman, and A. I. Larkin, *Phys. Rev. Lett.* **64**, 88 (1989).
- <sup>11</sup>T. Yildirim, A. B. Harris, and E. F. Shender, *Phys. Rev. B* **58**, 3144 (1998).
- <sup>12</sup>J.-P. Ader, *Phys. Rev. B* **65**, 014411 (2001).
- <sup>13</sup>A. N. Ignatenko, A. A. Katanin, and V. Yu. Irkhin, *JETP Lett.* **87**, 642 (2008).
- <sup>14</sup>L. M. Sandratskii, *Adv. Phys.* **47**, 91 (1998).
- <sup>15</sup>F. J. Pinski, J. Staunton, B. L. Gyorffy, D. D. Johnson, and G. M. Stocks, *Phys. Rev. Lett.* **56**, 2096 (1986).
- <sup>16</sup>M. Matsuura, Y. Endoh, H. Hiraka, K. Yamada, A. S. Mishchenko, N. Nagaosa, and L. V. Solovyeu, *Phys. Rev. B* **68**, 094409 (2003).
- <sup>17</sup>W. Pepperhoff and M. Acet, *Constitution and Magnetism of Iron and its Alloys* (Springer, Berlin, 2001).
- <sup>18</sup>A. I. Liechtenstein, M. I. Katsnelson, V. P. Antropov, and V. A. Gubanov, *J. Magn. Magn. Mater.* **67**, 65 (1987).
- <sup>19</sup>A. V. Ruban and H. L. Skriver, *Comput. Mater. Sci.* **15**, 119 (1999).
- <sup>20</sup>I. A. Abrikosov and H. L. Skriver, *Phys. Rev. B* **47**, 16532 (1993).
- <sup>21</sup>A. V. Ruban, S. I. Simak, S. Shallcross, and H. Skriver, *Phys. Rev. B* **67**, 214302 (2003).
- <sup>22</sup>U. von Barth and L. Hedin, *J. Phys. C* **5**, 1629 (1972).
- <sup>23</sup>I. Turek, J. Kudrnovsky, G. Bihlmayer, and S. Blügel, *J. Phys.: Condens. Matter* **15**, 2771 (2003).
- <sup>24</sup>S. Khmelevskiy, T. Khmelevska, A. V. Ruban, and P. Mohn, *J. Phys.: Condens. Matter* **19**, 326218 (2007).
- <sup>25</sup>I. Turek, J. Kudrnovsky, M. Divis, P. Franek, G. Bihlmayer, and S. Blügel, *Phys. Rev. B* **68**, 224431 (2003).
- <sup>26</sup>M. S. S. Brooks, L. Nordström, and B. Johansson, *J. Phys.: Condens. Matter* **3**, 2357 (1991).
- <sup>27</sup>R. Ahuja, S. Auluck, B. Johansson, and M. S. S. Brooks, *Phys. Rev. B* **50**, 5147 (1994).
- <sup>28</sup>K. Maiti, M. C. Malagoli, E. Magnano, A. Dallmeyer, and C. Carbone, *Phys. Rev. Lett.* **86**, 2846 (2001).
- <sup>29</sup>S. Khmelevskiy, I. Turek, and P. Mohn, *Phys. Rev. B* **70**, 132401 (2004).